Effect of capping layer on interlayer coupling in synthetic spin valves

Kebin Li,[1] Jinjun Qiu,[1] Guchang Han,[1] Zaibing Guo,[1] Yuankai Zheng,[1] Yihong Wu,[1,2] and Jinshan Li[3]
[1]*Data Storage Institute, DSI Building, No. 5 Engineering Drive 1, Singapore 117608, Republic of Singapore*
[2]*Department of Electrical and Computer Engineering, National University of Singapore, Republic of Singapore*
[3]*Hitachi Global Storage Technologies, 5600 Cottle Road, Mail Stop: 7ZDA/14-2, San Jose, California 95193, USA*
(Received 28 April 2004; revised manuscript received 25 October 2004; published 27 January 2005)

The magnetic and transport properties of high quality synthetic spin-valves with the structure of Ta/NiFe/IrMn/CoFe/Ru/CoFe/NOL/CoFe/Cu/CoFe/CL were studied by using magnetoresistance measurements. Here Ti, Hf, and Al are used as the capping layer. It is found that both the thickness and materials properties of the capping layers can affect the interlayer coupling field. The interlayer coupling field oscillates weakly with respect to the thickness of the Ti and Hf capping layers. Extremely strong ferromagnetic coupling has been observed when the thickness of the Al capping layer is in a certain range where resonant exchange coupling takes place. The strength of the interlayer coupling is inversely proportional to the square of the thickness of the spacer. It is a typical characteristic of quantum size effect.

DOI: 10.1103/PhysRevB.71.014436 PACS number(s): 72.15.Gd, 75.30.Et

I. INTRODUCTION

Spintronics offers opportunities for a new generation of devices combining conventional microelectronics with spin-dependent effects that arise from spin-charge interaction of the carriers. One of the major challenges in this field of spintronics is to control the dynamics of both carrier charge and spin by external electric and magnetic fields.[1,2] In spin-based electronic devices, such as read head sensors and magnetic random access memories,[3–5] one of the key issues is to manipulate the spin orientation of two ferromagnets (FMs) separated by one metallic or nonmetallic spacer. The interlayer magnetic coupling between two FM layers across the spacer oscillates with the thickness of the spacer.[6–8] The electronic origin for this oscillatory magnetic coupling is attributed to quantum interferences due to spin-dependent confinement of electrons in the spacer layer.[9–11]

Since the electrons are confined in the nonmagnetic cap layer (CL) due to the vacuum barrier, the interlayer exchange coupling (IEC) oscillates with the CL thickness, which is predicated theoretically by Bruno[12] and confirmed by experimental works done by Bounouh *et al.* on the Au/Co/Au/Co/Au(111) system,[13] by de Vries *et al.* on the Cu/Co/Cu/Co/Cu(001) system,[14] and by Okuno and Inomata on the Au/Fe/Au/Fe/Au(001) system.[15] To our best knowledge, so far there is no similar report in synthetic spin valves in which some in-active layers such as the seed layer, the structural guide layer and the antiferromagnetic layer may be responsible for weakening the confinement of the electrons.

A nano-oxide layer (NOL) inside the pinned layer can smoothen the surface of the interface and enhance the specular reflective coefficient, which leads to enhancement of the magnetoresistance effect and oscillation of the interlayer coupling field (H_{int}) with the thickness of the spacer observed in spin valves by many research groups.[16–19] It is expected that the effect of the electron confinement in the cap layer on the interlayer coupling should be observable in NOL-added synthetic spin valves. Here we will demonstrate that the interlayer coupling field between the free and pinned FM layers in NOL-added spin valves depends on the thickness of the cap layer and also the material properties of the cap layer. Because of the strong quantum confinement of the electrons, resonant exchange coupling has been observed in the system when Al is used as the cap layer. The strength of the interlayer coupling is inversely proportional to the square of the thickness of the spacer, indicating that the observed strong interlayer coupling field between the free and pinned layers is the nature of the quantum size effect of the cap layer.

II. EXPERIMENT

Synthetic spin valves (SVs) with a typical structure of Ta/NiFe/IrMn/CoFe/Ru/CoFe/NOL/CoFe/Cu/CoFe/CL (here, NOL stands for CoFe–O, and CL stands for cap layer, Al/Al–O or Ti/Ti–O and Hf/Hf–O) were grown on Si substrate coated with thermally oxidized 1 μm thick SiO_2 by using magnetron sputtering method under ultra high vacuum with base pressure of about 5×10^{-10} Torr. Here, Ta is used as the seed layer. NiFe is used as the structural guide layer, and IrMn is used as the antiferromagnetic layer. The compositions of the alloy targets are $Ni_{81}Fe_{19}$, $Ir_{20}Mn_{80}$, and $Co_{90}Fe_{10}$ (in atomic percentage), respectively. During deposition of the magnetic layers, an electrical-magnetic field with strength of 100 Oe was applied in order to induce the easy axis of the ferromagnetic layer. More detailed deposition conditions can be found in Refs. 16 and 20. Here we just summarize the formation of nano-oxide layer briefly. After deposition of Ta/NiFe/IrMn/CoFe/Ru/CoFe, the wafer was transferred to a plasma oxidation chamber to form a nano CoFe–O layer by exposing the CoFe metallic layer to pure oxygen at pressure of 3×10^{-3} Pa for 60 s. After that, the wafer was transferred back to the processing chamber for deposition of the rest part of the spin valves. Al-O, Ti-O, and Hf-O were naturally formed by exposing the fresh cap metallic layer to air after finishing deposition of the whole stack of thin film. After completion of the whole stack of

SVs, the samples were magnetically annealed at 235 °C at 1 T for 2 h. The magnetic field was along the easy axis of the ferromagnetic layer, so that the magnetization direction of the pinned layer was set by exchanging coupling between the ferromagnetic CoFe and the antiferromagnetic IrMn layer. Magnetoresistance (MR) measurements were carried out by using a four-probe method in a vibrated sample magnetometer with MR measurement fixture. X-ray diffraction (XRD) was used to characterize the structure of the thin films. XRD patterns show that the SVs are of (111) textural structure.

III. RESULTS AND DISCUSSIONS

A. The effect of Hf, Ti capping layers on the interlayer coupling field

A typical *R-H* curve measured on a SV with the structure of $Ta_3/NiFe_2/IrMn_8/CoFe_2/Ru_{0.8}/CoFe_1/NOL/CoFe_{2.3}/Cu_{2.3}/CoFe_{2.6}/AlO$ is shown in Fig. 1(a) in the field range from −6000 to 6000 Oe. When the strength of the field is larger than 6000 Oe, the magnetization of all the magnetic layers is in the positive direction, the resistance is at the lowest state. When the strength of the field is decreased, the magnetization of the pinned layer that is nearer to the free layer starts rotating to the negative direction and the resistance is increased. The resistance is at the highest state when the magnetization of the pinned layer is antiparallel to that of the free layer. When the external magnetic field is further decreased (smaller than $H_{\text{int}}-H_c$, $H_{\text{int}}>H_c$) or increased in the negative direction (larger than H_c-H_{int}, $H_c>H_{\text{int}}$), the magnetization of the free layer switches to the negative direction, so the resistance becomes the smallest again. Here H_c is defined as the coercivity of the free layer, and H_{int} is defined as the interlayer coupling field which stands for the offset field of the center of the minor MR loop caused by the magnetization switching of the free layer, as shown in the inset of Fig. 1(a). It is ferromagnetic coupling, when the minor magnetoresistance loop shifts to the same direction of the major magnetoresistance loop of the pinned layer as observed in this SV. It is antiferromagnetic coupling when the minor magnetoresistance loop shifts to the opposite direction of the major magnetoresistance loop of the pinned layer.

Figure 1(b) shows H_{int} as a function of the thickness of the Ti layer for a series of SVs with the structure of $Ta_3/NiFe_2/IrMn_8/CoFe_2/Ru_{0.8}/CoFe_1/NOL/CoFe_{2.3}/Cu_{2.3}/CoFe_{2.6}/Ti(t)/TiO$ (thicknesses of each layer are in nanometers). H_{int} was obtained based on magnetoresistance measurement of the SVs similar to the one shown in Fig. 1(a). Some data points shown in Fig. 1(b) were measured on samples with the fixed thickness of the cap layer (but not in the same batch) for three times. The data points shown in Fig. 1(b) are quite scattered. It is probably due to the thickness fluctuation of other layers such as the spacer and the free/pinned ferromagnetic layers. However, one still can find the trend that the interlayer coupling field oscillates weakly with respect to the thickness of Ti layer with a period of about 1.0 nm. Figure 1(c) shows H_{int} as a function of the thickness of Hf for a series of SVs with the structure of $Ta_3/NiFe_2/IrMn_8/CoFe_2/Ru_{0.8}/CoFe_1/NOL/CoFe_{2.3}/Cu_{2.3}/CoFe_{2.6}/Hf(t)/HfO$. Again the data are very scattered, but the trend is still there; H_{int} oscillates weakly with respect to the thickness of the Hf cap layer in a period of about 1.2 nm.

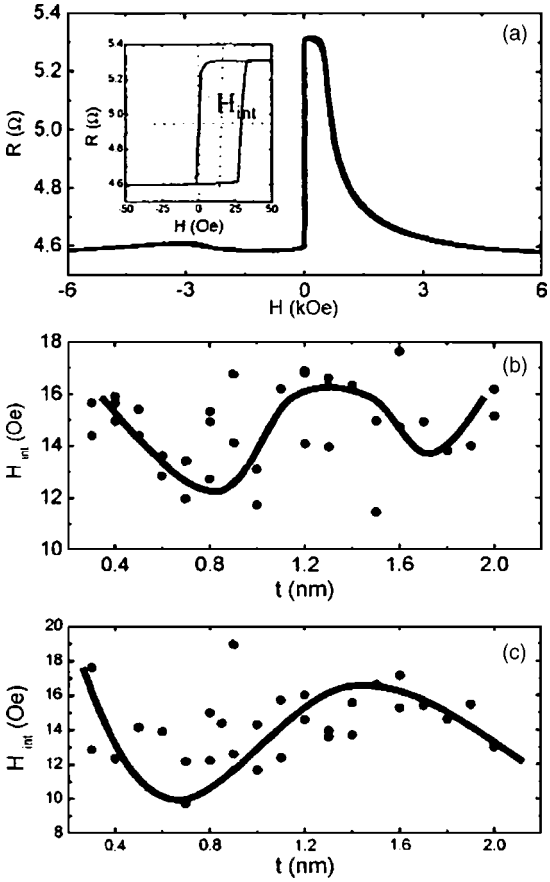

FIG. 1. (a) *R-H* curve for a typical SV with structure of $Ta_3/NiFe_2/IrMn_8/CoFe_2/Ru_{0.8}/CoFe_1/NOL/CoFe_{2.3}/Cu_{2.3}/CoFe_{2.6}/AlO$. The inset shows the *R-H* curve for the minor loop in which the interlayer coupling field (H_{int}) is defined. (b) shows H_{int} as a function of the thickness of Ti for a series of SVs with the structure of $Ta_3/NiFe_2/IrMn_8/CoFe_2/Ru_{0.8}/CoFe_1/NOL/CoFe_{2.3}/Cu_{2.3}/CoFe_{2.6}/Ti(t)/TiO$. (The solid line is used for eye-guidance only.) (c) shows H_{int} as a function of the thickness of *Hf* for a series of SVs with the structure of $Ta_3/NiFe_2/IrMn_8/CoFe_2/Ru_{0.8}/CoFe_1/NOL/CoFe_{2.3}/Cu_{2.3}/CoFe_{2.6}/Hf(t)/HfO$. (The solid line is used for eye-guidance only.)

The electronic origin for the oscillation of the interlayer coupling is due to the density of states oscillations because of electron confinement in the spacer. The interlayer coupling oscillation period is determined by the beating frequency between the Fermi wavelength and the lattice constant, namely the envelope function wave vector k_{env} by subtracting the Fermi wave vector $k_F=2\pi/\lambda_F$ from the Brillouin zone boundary wave vector k_{ZB}:

$$k_{\text{env}} = k_{ZB} - k_F. \tag{1}$$

Hf and Ti are of hcp structure $a=3.20$ Å, $c=5.07$ Å for Hf and $a=2.95$ Å, $c=4.69$ Å for Ti. The maximum Fermi velocity of Hf is about 0.667×10^6 m/s and 0.569×10^6 m/s

for Ti.[21] According to Eq. (1), the oscillation period of the interlayer coupling for the Hf cap layer is about 7.74 for (1000) and 4.73 Å for (0002); it is about 5.48 Å for Ti(1000) and 3.69 Å for Ti(0002). In terms of the oscillation period, the experimental results are not in agreement with the theoretical estimation. It may be due to the following two reasons. One of them is that the Hf and Ti cap layers deposited in the SVs are polycrystalline instead of single crystals that are assumed in the theoretical estimation. Second, the interlayer coupling field between the free and pinned FM layers in the SVs depends on many factors such as the thickness of each FM layer, the thickness of the spacer, the magnetic moment of the free layer, as well as the surface roughness of the spacer. The thickness fluctuation of any layer will affect the electron confinement in the cap layer, resulting in scattered data points, and will eventually smoothen the oscillation of the interlayer coupling field with respect to the thickness of the cap layer.

In order to provide more quantitative analysis, we simplify the synthetic SVs with the NOL in the pinned layer into four layers with one barrier in the pinned layer and one barrier on top of the cap layer. The simplified one-dimensional potential for the system can be modeled as shown in Fig. 2. $L1$ and $L2$ are the pinned CoFe and free CoFe layer thickness, D and T are the spacer and the cap layer thickness. The NOL layer and top oxide cap layer are simplified by two potential barriers with height of W. Electrons of both spin directions in Cu and spin-up electrons in CoFe have Fermi wave vector k_F; spin down electrons in CoFe have wave vector $k_F^{\downarrow}$. Electrons of both spin directions in the cap layer have Fermi wave vector k_F'. The reflection coefficient at the interface between Cu and CoFe as well as between CoFe and the cap layer is simplified as $r_\infty=(k_F-k_F^{\downarrow})/(k_F+k_F^{\downarrow})$. The reflection coefficient of electrons of both spin directions at the interface between CoFe and the NOL barrier or between the cap layer and the cap oxide barrier is simplified as $r_v=(k_F'-ik_v)/(k_F'+ik_v)$ with

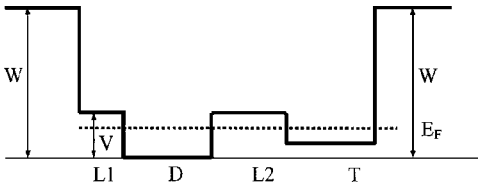

FIG. 2. Illustration of a simplified one-dimensional potential modeled for the nano-oxide-added synthetic SVs with metallic cap layers.

$$\frac{h^2k_v^2}{8\pi^2m}=W-\varepsilon. \tag{2}$$

Within the free electron approximation of Bruno's model,[12] we can derive the equation for the bilinear interlayer coupling strength J_1 in the limit of weak confinement (small r_∞):

$$\begin{aligned}J_1=\frac{1}{2}(E_F-E_{AF})=\frac{h^2k_F^2}{4\pi^4m}\,\mathrm{Im}\left(e^{2ik_FD}\int_0^{+\infty}dkk\Delta r_A\Delta r_Be^{-2kD}\right)=\frac{h^2}{64\pi^4m}\,\mathrm{Im}\Bigg[r_\infty^2\Bigg(e^{2ik_FD}\left(\frac{D}{k_F}\right)^{-2}-e^{2ik_F^{\downarrow}L_2+2ik_FD}\left(\frac{L_2}{k_F^{\downarrow}}+\frac{D}{k_F}\right)^{-2}\\
-e^{2ik_F^{\downarrow}L_1+2ik_FD}\left(\frac{L_1}{k_F^{\downarrow}}+\frac{D}{k_F}\right)^{-2}+e^{2ik_F^{\downarrow}(L_2+L_1)+2ik_FD}\left(\frac{L_1+L_2}{k_F^{\downarrow}}+\frac{D}{k_F}\right)^{-2}\Bigg)-r_\infty r_\gamma\Bigg(e^{2ik_FL_1+2ik_FD}\left(\frac{L_1}{k_F}+\frac{D}{k_F}\right)^{-2}\\
-e^{2ik_FL_1+2ik_F^{\downarrow}L_2+2ik_FD}\left(\frac{L_1}{k_F}+\frac{L_2}{k_F^{\downarrow}}+\frac{D}{k_F}\right)^{-2}+e^{2ik_F'T+2ik_FL_2+2ik_FD}\left(\frac{T}{k_F'}+\frac{L_2}{k_F}+\frac{D}{k_F}\right)^{-2}-e^{2ik_F'T+2ik_F^{\downarrow}L_2+2ik_FD}\left(\frac{T}{k_F'}+\frac{L_2}{k_F^{\downarrow}}+\frac{D}{k_F}\right)^{-2}\\
-e^{2ik_F'T+2ik_FL_2+2ik_F^{\downarrow}L_1+2ik_FD}\left(\frac{T}{k_F'}+\frac{L_1}{k_F^{\downarrow}}+\frac{L_2}{k_F}+\frac{D}{k_F}\right)^{-2}+e^{2ik_F'T+2ik_F^{\downarrow}L_2+2ik_F^{\downarrow}L_1+2ik_FD}\left(\frac{T}{k_F'}+\frac{L_1}{k_F^{\downarrow}}+\frac{L_2}{k_F^{\downarrow}}+\frac{D}{k_F}\right)^{-2}\Bigg)\\
+r_\gamma^2\Bigg(e^{2ik_FL_1+2ik_F'T+2ik_FL_2+2ik_FD}\left(\frac{T}{k_F'}+\frac{L_2}{k_F}+\frac{L_2}{k_F}+\frac{D}{k_F}\right)^{-2}-e^{2ik_FL_1+2ik_F'T+2ik_F^{\downarrow}L_2+2ik_FD}\left(\frac{T}{k_F'}+\frac{L_2}{k_F^{\downarrow}}+\frac{L_1}{k_F}+\frac{D}{k_F}\right)^{-2}\Bigg)\Bigg].\end{aligned} \tag{3}$$

The first line in Eq. (3) corresponds to the case of a semi-infinite overlayer and semi-infinite pinned layer, in the absence of the cap oxide barrier and NOL potential barrier. The remaining terms represent the effect of confinement due to the oxide potential barrier at each side. By using $k_F=1.36$ Å^{-1}, $k_F^{\downarrow}=1.26$ Å^{-1}, $L1=2.3$ nm, $L2=2.6$ nm, $D=2.3$ nm, $W=5.0$ eV, basically we can calculate the interlayer coupling field as a function of the thickness of the cap layer. The calculated oscillation period is about 0.5 nm, which is in good agreement with the estimated value mentioned early. The oscillation amplitude is about 5 to 6 Oe, which is in good agreement with our experimental results. However, our experimental data are very scattered when we put the data points of different batch samples in the same plot. According to Eq. (3), the interlayer coupling field oscillates with the thickness of the spacer, the thickness of the free/pinned FM layers, and also the thickness of the cap layer. Any thickness fluctuation of these layers will influence the interlayer coupling field. Such kind of thickness fluctuation is unavoidable during the sample preparation, especially

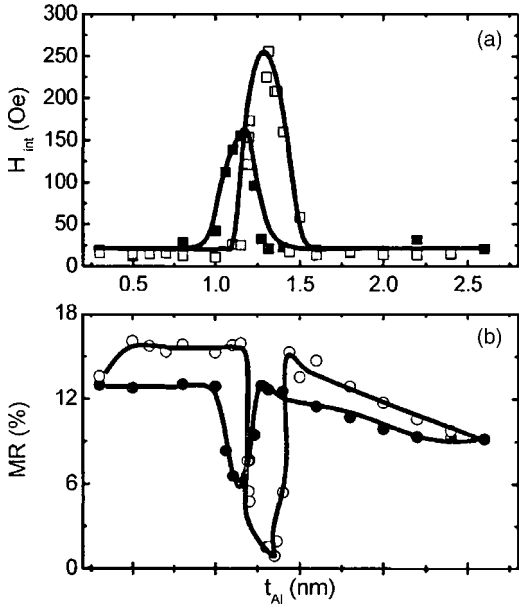

FIG. 3. (a) H_{int} and (b) MR as a function of the thickness of Al cap layer for two series of samples with the structure of $Ta_3/NiFe_2/IrMn_8/CoFe_2/Ru_{0.8}/CoFe_1/NOL/CoFe_{2.3}/Cu_{2.3}/CoFe_{2.6}/Al(t)/AlO$ (open symbols) and $Ta_3/NiFe_2/IrMn_8/CoFe_2/Ru_{0.8}/CoFe_3/Cu_{2.3}/CoFe_{2.6}/Al(t)/AlO$ (solid symbols). (The solid lines are used for eye-guidance only.)

for the samples from one batch to another batch that are prepared by the magnetron sputtering method. It is probably the main reason that makes the oscillation blur.

B. Abnormal enhancement of interlayer coupling in NOL SVs with Al used as the cap layer

Figure 3(a) shows the interlayer coupling field as a function of the thickness of the cap Al layer for a series of SVs with the structure of $Ta_3/NiFe_2/IrMn_8/CoFe_2/Ru_{0.8}/CoFe_1/NOL/CoFe_{2.3}/Cu_{2.3}/CoFe_{2.6}/Al(t)/AlO$. The open squares are for H_{int} that is a function of the thickness of the cap Al layer in a series of synthetic SVs with CoFe–O nano-oxide layer inside the pinned CoFe layer. There is an abnormally strong interlayer coupling occurring at 1.3 nm of the Al cap layer. The maximum of H_{int} increases up to 250 Oe which is about 50 times larger than that obtained in an usual NOL-added SV. The full width of the half maximum peak is about 0.3 nm, which means only about one atomic monolayer difference of Al thickness can cause ten times difference in the interlayer coupling field. It is very obvious that it should be attributed to the quantum size effect. The small oscillation peak of the interlayer coupling field with respect to the thickness of the cap layer is now covered by this huge interlayer coupling field peak. Since this interlayer coupling peak does not oscillate with respect to the thickness of the cap layer, it cannot be interpreted by Eq. (3) within the frame of the free electron model. It is believed that it should be associated with the resonant exchange coupling because of the quantum-size effect and the interference of conducting electrons in the spacer and cap layer quantum wells. Due to the confinement of the cap layer surface with an infinite oxide barrier height, the conducting electrons are subject to the spin-dependent reflection from surfaces and interfaces, so they could interfere in the quantum wells of the cap layer, setting up the spin-dependent quantum well states. Under certain conditions, this kind of interference becomes maximum, so the resonant exchange coupling takes place. The resonant exchange coupling between two ferromagnets separated by a nonmetallic spacer has been theoretically addressed by Wang *et al.*[22]

The strong ferromagnetic resonant coupling observed in the nano-oxide-added synthetic spin valves with Al cap layer is due to strong confinement of the conducing electrons in the quantum well of the cap layer because of the enhancement of the reflection of electrons between the nano-oxide CoFe-O barrier in the pinned layer and the cap oxide barrier on top of the metallic cap layer. This quantum size effect can be verified by the following experiment. Since the quantum interference of the electron is formed when the electron reflects back and forth between the nano-oxide pinned layer and the insulator potential barrier on top of the cap layer, it is expected that the resonant coupling will become weak when the nano-oxide CoFe-O layer inside the pinned layer is removed from the structure. As illustrated by the solid squares (the solid lines serve for eye-guidance only) in Fig. 3(a), the maximum of the interlayer coupling field is reduced from 256 to 153 Oe, in the series of SVs with the structure of $Ta_3/NiFe_2/IrMn_8/CoFe_2/Ru_{0.8}/CoFe_3/Cu_{2.3}/CoFe_{2.6}/Al(t)/AlO$. Interestingly, the peak position shifts from 1.3 to 1.2 nm, and it is very sensitive to the thickness of the cap layer. The shift of the peak position is due to the phase shift of the wave functions of electrons after reflection at the interface between the pinned CoFe and the CoFe-O nano-oxide barrier. The reduction of H_{int} is due to the weaker reflection of the electrons when there is no nano-oxide CoFe-O layer inside the pinned layer.

Since the magnetoresistance effect correlates with the interlayer coupling in SVs, such kind of quantum interference effect can be remarkably observed in the magnetoresistance effect. Figure 3(b) shows the MR ratio as a function of the thickness of the cap layer for two series of samples with the structure of $Ta_3/NiFe_2/IrMn_8/CoFe_2/Ru_{0.8}/CoFe_1/NOL/CoFe_{2.3}/Cu_{2.3}/CoFe_{2.6}/Al(t)/AlO$ (open circles) and $Ta_3/NiFe_2/IrMn_8/CoFe_2/Ru_{0.8}/CoFe_3/Cu_{2.3}/CoFe_{2.6}/Al(t)/AlO$ (solid circles). With CoFe-O NOL inside the pinned layer, MR is larger in the whole range of the cap layer investigated except for the resonant regime. It is because of the enhancement of the specular reflection of electrons at the interface of CoFe-O NOL and at the interface of the top AlO layer. The magnetic coupling between the free and pinned ferromagnetic layers is strongly ferromagnetic coupled at the resonant condition, as a result, MR is minimum at this regime. The stronger the coupling field, the smaller the MR ratio. MR is suppressed from about 16% to zero when the CoFe-O NOL is inside the pinned CoFe layer. However, MR drops from 12% to about 5% if there is no CoFe-O NOL inside the pinned CoFe layer.

The transport properties are in good agreement with the magnetic properties of the system. The magnetoresistance effect is strongly correlated with the interlayer coupling. As an example, Fig. 4(a) shows *MR-H* curve for a SV with the

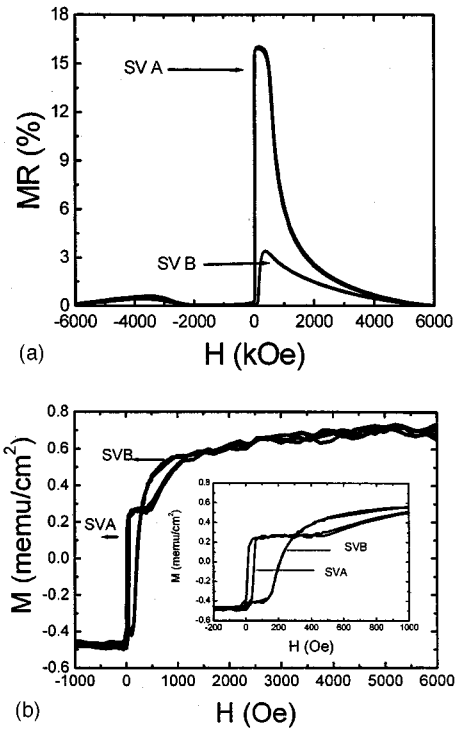

FIG. 4. (a) *MR-H* curves and (b) *M-H* curves for a SV with the structure of $Ta_3/NiFe_2/IrMn_8/CoFe_2/Ru_{0.8}/CoFe_1/NOL/CoFe_{2.3}/Cu_{2.3}/CoFe_{2.6}/Al_{1.2}/AlO$ (SV B) and a spin valve with the structure of $Ta_3/NiFe_2/IrMn_8/CoFe_2/Ru_{0.8}/CoFe_1/NOL/CoFe_{2.3}/Cu_{2.3}/CoFe_{2.6}/Al_{1.6}/AlO$ (SV A).

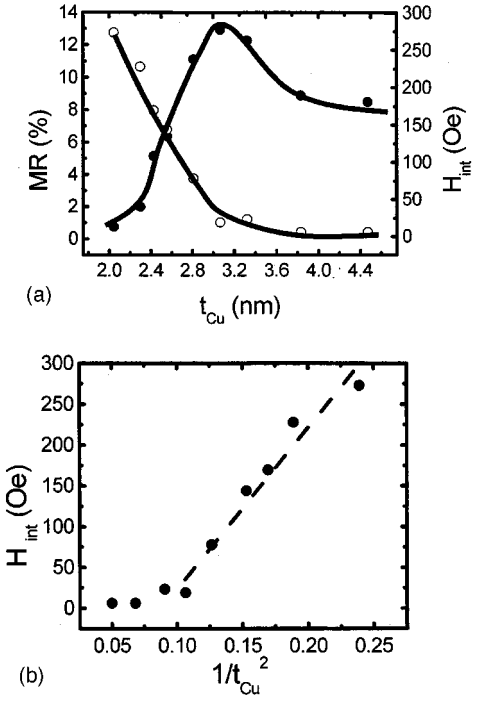

FIG. 5. (a) MR and H_{int} as a function of the thickness of the spacer for a series of SVs with the structure of $Ta_3/NiFe_2/IrMn_8/CoFe_2/Ru_{0.8}/CoFe_1/NOL/CoFe_{2.3}/Cu(t)/CoFe_{2.6}/Al_{1.2}/AlO$ (open circles are for H_{int} and solid circles are for MR). (b) Plot of H_{int} as a function of $1/t_{Cu}^2$ based on the data plotted in (a).

structure of $Ta_3/NiFe_2/IrMn_8/CoFe_2/Ru_{0.8}/CoFe_1/NOL/CoFe_{2.3}/Cu_{2.3}/CoFe_{2.6}/Al_{1.2}/AlO$ (SV B), the thickness of Al is about 1.2 nm, which is in the vicinity of the giant interlayer coupling peak. So the interlayer coupling is about 220 Oe, and the MR ratio is very small, only about 1.6%. Figure 4(a) also shows the *MR-H* curve for a SV with the structure of $Ta_3/NiFe_2/IrMn_8/CoFe_2/Ru_{0.8}/CoFe_1/NOL/CoFe_{2.3}/Cu_{2.3}/CoFe_{2.6}/Al_{1.6}/AlO$ (SV A); the thickness of the Al is about 1.6 nm, which is out of the giant peak range, so the MR ratio is large, about 14.9%, and the interlayer coupling field is only about 20 Oe. To confirm the correlation between the interlayer coupling and the MR ratio, we have also measured their *M-H* curves as shown in Fig. 4(b). The inset of Fig. 4(b) shows the part of the *M-H* curve in the range from −200 to 1000 Oe. In the former case, the spin orientation of the free layer and the pinned layer is strongly ferromagnetic coupled; the *M-H* curve is caused by the rotation of the free layer and the pinned layer together. But for the latter case, the *M-H* curve for the free layer is well separated from the *M-H* curve of the pinned layer. The interlayer coupling field determined by *M-H* curves is in good agreement with the value determined by *R-H* curves. H_{int} also depends on the moment of the free layer provided that the interlayer coupling energy is a constant. The smaller the moment of the free layer, the larger the H_{int}. Look at the *M-H* curve shown in Fig. 4(b). The total moment of the free and pinned layers is almost the same for SV B and SV A within our measurement accuracy although the feature of their *M-H* curves is quite different. That means the moment fluctuation in the free layer (if there is any) is not able to account for ten times' enhancement of the H_{int} observed in SV B.

Basically there are three types of interlayer coupling,[23] namely, "orange peel" coupling, domain wall exchange coupling, and quantum exchange coupling, which is due to the electron confinement. The "orange peel" type ferromagnetic coupling due to magnetostatic coupling arises due to interactions between free poles which are setup at topographically conformal, uneven interfaces. The strength of the "orange peel" coupling is exponential decay with increasing thickness of the spacer. The domain wall exchange coupling is caused by the interaction of the stray field generated from the domain wall of the free and pinned FM layers. However, the interlayer coupling induced by the domain wall coupling is characteristic of the antiferromagnetic property, which is not the case observed in our experiments. The quantum exchange coupling is the nature of the quantum size effect. One of the characteristics of this type of exchange coupling is that the strength of the interlayer coupling field should be inversely proportional to the square of the thickness of the spacer. To this end, we have also fabricated a series of spin valves with the structure of $Ta_3/NiFe_2/IrMn_8/CoFe_2/Ru_{0.8}/CoFe_1/NOL/CoFe_{2.3}/Cu(t)/CoFe_{2.6}/Al_{1.2}/AlO$ by changing the thickness of the spacer. Here the thickness of Al is fixed at 1.2 nm, around which the interlayer coupling is near to the maximum. As shown in Fig. 5(a), the interlayer coupling field decreases while the MR ratio is gradually in-

creased with increasing thickness of the spacer. If the interlayer coupling field is replotted as a function of the $1/t_{Cu}^2$, as shown in Fig. 5(b), it is found that H_{int} is linear to $1/t_{Cu}^2$. This indicates that H_{int} is inversely proportional to the square of the thickness of the spacer. This is exactly what the quantum size effect predicates. With further increasing the thickness of the spacer layer, the MR ratio decreases again while the interlayer coupling is almost saturated. The decreasing of the MR ratio with increasing the thickness of the spacer (above 3.2 nm) is probably due to the current shunting effect in the spacer.

IV. SUMMARY

In summary, very weak oscillations of the interlayer coupling with respect to the thickness of the cap layer have been observed in nano-oxide-added synthetic SVs although the data are quite scattered due to the thickness fluctuation of the spacer and free/pinned FM layers in the samples. The origin of oscillations of the interlayer coupling can be interpreted by the quantum interference effect of the wave functions of free electrons confined in the quantum wells of the spacer and the cap layer. The resonant interlayer exchange coupling can take place when Al is used as the cap layer if the resonant condition can be setup. Since the magnetoresistance is correlated to the interlayer coupling, magnetoresistance effect is almost quenched at the thickness of the cap layer where the resonant ferromagnetic exchange coupling takes place. Although it is unable to be explained by the free electron model, our experimental evidences show that it should be attributed to the quantum size effect. From an application point of view, it needs to avoid such kind of strong ferromagnetic coupling between the free and pinned layers. But from a scientific point of view, our experimental results have demonstrated that it can offer us an alternative way to manipulate the magnetic interaction between two ferromagnets separated by a metallic spacer just by engineering the wave functions of electrons.

[1] S. A. Wolf, D. D. Awschalom, R. A. Buhrman, J. M. Daughton, S. von Molnár, M. L. Roukes, A. Y. Chtchelkanova, and D. M. Treger, Science **294**, 1488 (2001).

[2] S. D. Sarma, Nature (London) **2**, 292 (2003).

[3] C. Tsang *et al.*, IEEE Trans. Magn. **30**, 3801 (1994).

[4] J. Daughton, J. Brown, R. Beech, A. Pohm, and W. Kude, IEEE Trans. Magn. **30**, 4608 (1994).

[5] G. Prinz, Science **282**, 1660 (1998).

[6] P. Grünberg, R. Schreiber, Y. Pang, M. B. Brodsky, and H. Sowers, Phys. Rev. Lett. **57**, 2442 (1986).

[7] S. S. P. Parkin, N. More, and K. P. Roche, Phys. Rev. Lett. **64**, 2304 (1990).

[8] S. S. P. Parkin, R. Bhadra, and K. P. Roche, Phys. Rev. Lett. **66**, 2152 (1991).

[9] F. J. Himpsel, J. E. Ortega, G. J. Mankey, and R. F. Willis, Adv. Phys. **47**, 511 (1998).

[10] R. K. Kawakami, E. Rotenberg, H. J. Choi, E. J. Escorcia-Apricio, M. O. Bowen, J. H. Wolfe, E. Arenholz, Z. D. Zhang, N. V. Smith, and Z. Q. Qiu, Nature (London) **398**, 132 (1999).

[11] Z. Q. Qiu and N. V. Smith, J. Phys.: Condens. Matter **14**, R169 (2002).

[12] P. Bruno, J. Magn. Magn. Mater. **164**, 27 (1996).

[13] A. Bounouh, P. Beauvillain, P. Bruno, C. Chappert, R. Mégy, and P. Veillet, Europhys. Lett. **33**, 315 (1996).

[14] J. J. de Vries, A. A. P. Schudelaro, R. Jungblut, P. J. H. Bloemen, A. Reinders, J. Kohlhepp, R. Coehoorn, and W. J. M. de Jonge, Phys. Rev. Lett. **75**, 4306 (1995).

[15] S. N. Okuno and K. Inomata, J. Phys. Soc. Jpn. **64**, 3631 (1995).

[16] K. Li, Y. Wu, J. Qiu, G. Han, Z. Guo, H. Xie, and T. C. Chong, Appl. Phys. Lett. **79**, 3663 (2001).

[17] J. Hong and H. Knal, J. Appl. Phys. **93**, 2095 (2003).

[18] J. Hong, J. Kane, J. Hashiimoto, M. Yamagishi, K. Nama, and H. Kanai, IEEE Trans. Magn. **38**, 15 (2002).

[19] T. Lin and D. Mauri, Appl. Phys. Lett. **78**, 2181 (2001).

[20] K. Li, Y. Wu, J. Qiu, and T. C. Chong, J. Appl. Phys. **91**, 8563 (2002).

[21] http://www. physik.tu-dresden.de/~fermisur/

[22] J.-Z. Wang, B.-Z. Li, and Z.-N. Hu, Phys. Rev. B **62**, 6570 (2000).

[23] C. L. Platt, M. R. McCartney, F. T. Parker, and A. E. Berkowitz, Phys. Rev. B **61**, 9633 (2000).